Cone Beam Computed Tomography 3D Reconstruction of the Mandibular Condyle

Brian Schlueter[a]; Ki Beom Kim[b]; Donald Oliver[c]; Gus Sortiropoulos[d]

ABSTRACT

Objective: To determine the ideal window level and width needed for cone beam computed three-dimensional (3D) reconstruction of the condyle.

Materials and Methods: Linear dimensions were measured with a digital caliper to assess the anatomic truth for 50 dry human mandibular condyles. Condyles were scanned with the i-CAT cone beam computed tomography (CBCT) and 3D-models were reconstructed. Three linear three-dimensional measurements were made on each of the 50 condyles at 8 different Hounsfield unit (HU) windows. These measurements were compared with the anatomic truth. Volumetric measurements were also completed on all 50 condyles, at 23 different window levels, to define the volumetric distribution of bone mineral density (BMD) within the condyle.

Results: Significant differences were found in two of the three linear measurement groups at and below the recommended viewing window for osseous structures. The most accurate measurements were made within the soft tissue range for HU window levels. Volumetric distribution measurements revealed that the condyles were mostly comprised of low-density bone, and that condyles exhibiting significant changes in linear measurements were shown to have higher percentages of low-density bone than those condyles with little change from the anatomic truth.

Conclusions: CBCT assessment of the mandibular condyle, using the 3D reconstruction, is most accurate when accomplished at density levels below that recommended for osseous examination. However, utilizing lower window levels which extend into the soft tissue range, may compromise one's capacity to view the bony topography.

KEY WORDS: Cone beam; TMJ

INTRODUCTION

Standard radiographic studies of the temporomandibular joint (TMJ) such as the plain film radiography and panoramic radiography, have little capacity to reveal anything more than gross osseous changes[1] within the joint. Therefore, in some cases a more comprehensive radiographic study is indicated.

Three-dimensional (3D) evaluations, such as computed tomography (CT) have been utilized to evaluate the TMJ. However, historically, high cost,[2,3] large radiation dosage,[4,5] large space requirements,[2,3] and the high level of skill required for interpretation have kept its use to a minimum. With the introduction of limited cone beam technology, such deterrents of CT imaging have been greatly diminished. With several cone beam computed tomography (CBCT) scanners now available, lower radiation dosages,[6–9] and lower costs,[2] 3D radiography is becoming more commonplace in the dental profession as it proves to be an valuable diagnostic tool.

Within the condyle, there is variation in bone density and composition. Cortical bone, trabeculae, and intertrabecular tissue have varying densities and mechanical properties.[10–14] These differences present a challenge when examining the bony subarticular surfaces of the condyle with 3D CT imaging. For computed tomography, density is often expressed in the form of CT numbers or Hounsfield units (HU).

[a] Private Practice, St Louis, Mo.
[b] Assistant Professor, Department of Orthodontics, Saint Louis University, St Louis, Mo.
[c] Assistant Professor, Department of Orthodontics, Saint Louis University, St Louis, Mo.
[d] Professor, Department of Orthodontics, Saint Louis University, St Louis, Mo.
Corresponding author: Dr Ki Beom Kim, Assistant Professor, Department of Orthodontics, Saint Louis University, 3320 Rutger Street, St Louis, MO 63104
(e-mail: kkim8@slu.edu)

Accepted: October 2007. Submitted: July 2007.

 DOI: 10.2319/072007-339.1

Hounsfield[15] originally described the HU as an absorption value, and he constructed a scale to demonstrate the accuracy to which the absorption values could be ascertained on a visual image. For the machine he described,[15] the scale ranged from air (−1000) at the bottom of the scale, to bone (1000) at the top of the scale. The range of tones between black and white seen in an image can be limited to a large or small window within the scale. This window can then be raised or lowered depending upon the absorption value of the material of interest.[15] The examiner must be able to decide what window level and width will most accurately represent the anatomic truth of a tissue under examination.

The purpose of the present study was to determine the ideal window width and level for the examination of the condyle, and, if these were identified, could one reliably evaluate the mandibular condyle using the CBCT 3D reconstruction?

MATERIALS AND METHODS

Selecting the Sample

The 25 dry human skulls in this study were used with the permission of The Department of Anatomical Science, Southern Illinois University at Edwardsville, School of Dental Medicine.

For each condyle, six anatomic landmarks were identified, marked, and photographed (Figure 1). Three linear measurements were made on the condyle including: height, width, and length (Table 1). All direct measurements were made by one operator using an electronic digital caliper (P.N. 50001, Chicago Brand, Fremont, Calif). Reproduction of the original landmark locations on the 3D renderings was assisted with photographs and markings on the condyles themselves.

Imaging

CBCT scans of the skulls were acquired with the i-CAT scanner (Imaging Sciences International, Hatfield, Pa). The device was operated at 120 kVp and 3–8 mA by using a high frequency generator with a fixed anode and a 0.5 mm focal spot. A single 40-second high-resolution scan was made of each skull. The voxel size was set at 0.25, providing the detail attainable with an i-CAT CBCT scanner.

Multiplanar reconstructions from the DICOM (Digital Imaging and Communications in Medicine) data were made using V-works 4.0 imaging software (Cybermed Inc, Seoul, Korea).

Isolating and Measuring the Condyle

Each of the 50 condyles was isolated prior to making 3D and volumetric measurements. Frankfort hori-

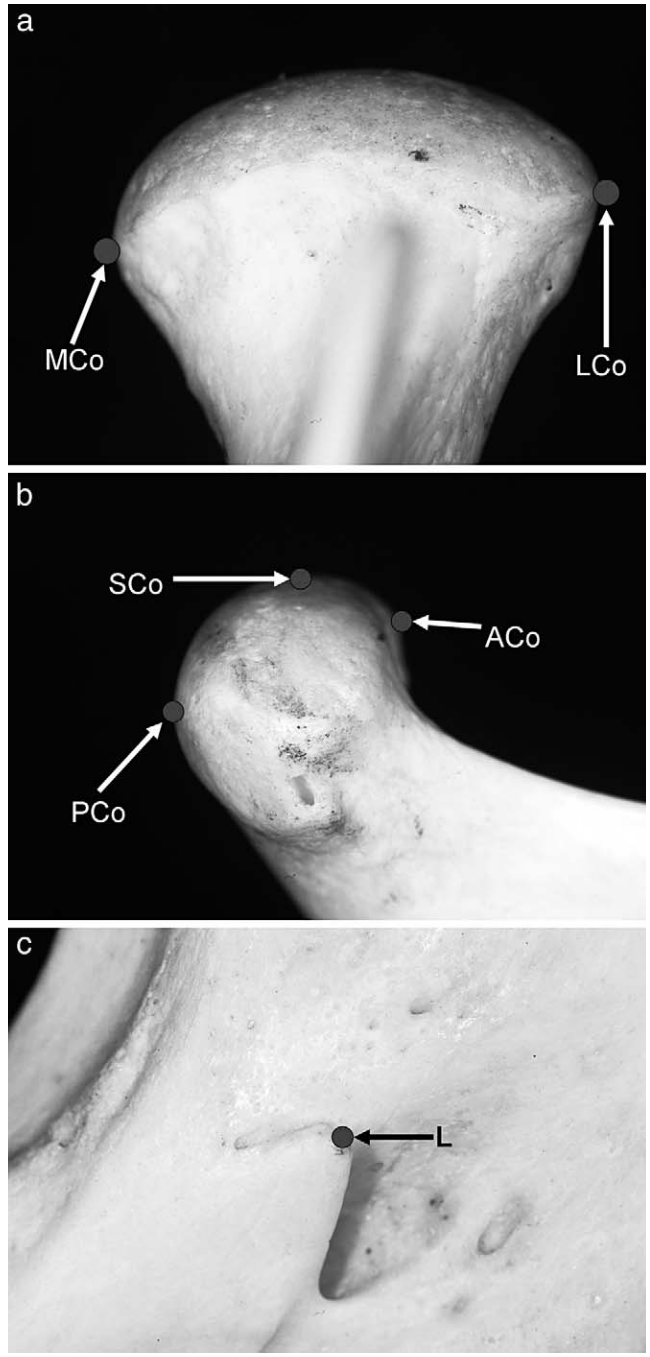

Figure 1. Anatomic landmarks: (a) anterior view of condyle showing medial mandibular condyle (MCo) and lateral mandibular condyle (LCo), (b) lateral view of condyle showing posterior mandibular condyle (PCo), anterior mandibular condyle (ACo), and superior mandibular condyle (SCo), and (c) lingual view of the ramus showing lingula (L).

zontal (FH) plane was constructed by creating a plane from the inferior orbital rim to the superior border of the external auditory meatus. An initial cut was made parallel to the FH plane just above the superior aspect of the condyle. The remaining surrounding structures

Table 1. Definitions of Condylar Linear Measurements

Measurement	Linear Distance	Definition
Condylar length (CL)	ACo – PCo	Linear distance between anterior mandibular condyle and posterior mandibular condyle
Condylar width (CW)	MCo – LCo	Linear distance between lateral mandibular condyle and medial mandibular condyle
Condylar height (CH)	SCo – L	Linear distance between superior mandibular condyle and lingula

were progressively removed using various sculpting tools (Figure 2).

Three-dimensional multiplanar reconstructions were produced for each of the eight window widths defined in Table 2. Condylar width (CW), condylar length (CL), and condylar height (CH) were measured. These landmarks and the measurements made using them are defined in Tables 1 and 3.

In the event of disappearance of portions of condylar anatomy due to variation in window widths, virtual planes are constructed. These planes are constructed perpendicular to the line of measurement.

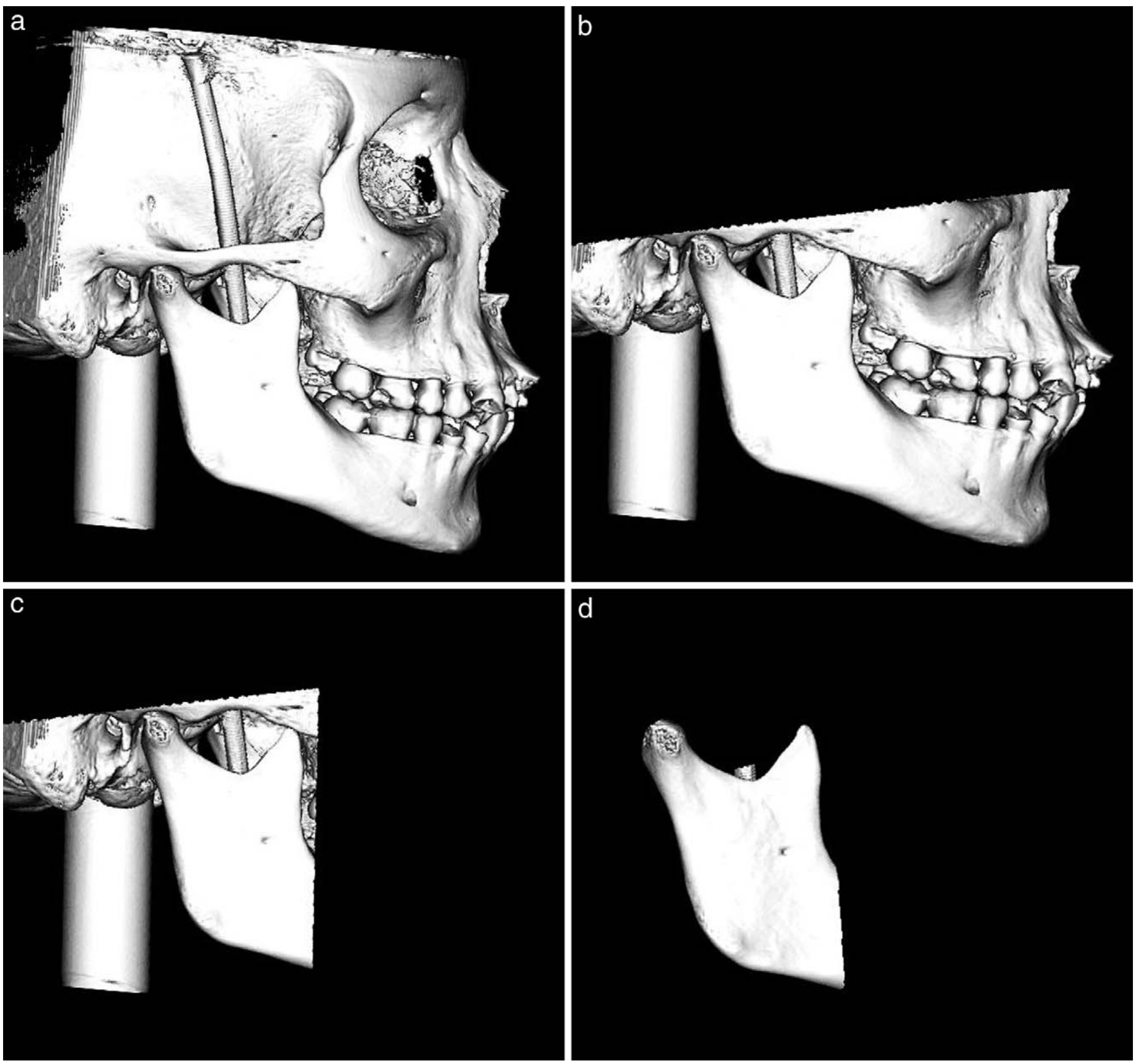

Figure 2. 3D reconstruction isolation: (a) initial lateral view 3D reconstruction, (b) Frankfort horizontal initial sculpting cut, (c) vertical sculpting cuts, and (d) completed isolation for condylar measurements.

Table 2. Hounsfield Unit Window Widths (W) Used to Create 3D Renderings of the Condyles. 3D Linear Measurements Were Accomplished on Each of These Renderings

Window Widths for 3D Linear Measurements	
W1	−524 to 2476 HU
W2	−424 to 2476 HU
W3	−324 to 2476 HU
W4	−224 to 2476 HU
W5	−124 to 2476 HU
W6	−24 to 2476 HU
W7	76 to 2476 HU
W8	176 to 2476 HU

Volume Measurements at Varying Window Widths

Prior to making volumetric measurements, a complete isolation of the condyle was completed. The final cut was made parallel to the FH plane at the level of the inferior point in the sigmoid notch. The isolation process for volumetric measurements is shown in Figure 3. After the isolation, volumetric measurements were made for each of the 23 window widths in order to define percentages of the condylar volume within each window. Each window represents a range of bone densities defined in the software as HU.

The first volumetric measurement was made at WW1 (176 to 275 HU), and each of the remaining 22 volumetric measurements were made in 99 HU width increments extending up to 2475 HU. One final volumetric measurement was made with the total range of 176 to 2475 HU (Table 4). WW24 (176 to 2475 HU) was used to find the total volume in the recommended bone density range from V-works.

Data Analysis

Differences between the 3D linear measurements and the gold standard measurements were calculated and analyzed using SPSS 14.0 (SPSS Inc, Rainbow Technologies, Chicago, Ill). Significance testing for 3D linear measurement differences was accomplished using independent *t*-tests with a 95% confidence interval. Linear measurement percent differences were calculated in the 176 to 2476 HU window for each of the 50 condyles. CW, CL, and CH were individually analyzed. The average percent linear measurement change was calculated for the 50 condyles in each measurement group. All percent changes were plotted on a distribution curve above and below the calculated means for CW and CL. The mean percent change was 18.38 for CL and 15.93 for CW. The distribution of numbers was segmented into the following groups: (1) numbers <10% into groups CW0 and CL0, (2) the numbers between 10% and 24% into the mean group and (3) numbers >24% into groups CW1 and CL1. The mean group range of condyles was excluded from the remainder of data analysis. The distributions of condyles in their respective ranges are shown in Figure 4. The percent volumes of the condyles in the outlying groups were compared using independent *t*-tests at each of the 23 volumetric window widths (WW) (Table 5). The CL0 and CL1 groups were plotted on a distribution curve to compare the distribution of bone volume in the two groups (Figure 5). The same was done for the CW0 and CW1 groups on a separate graph (Figure 6). Linear measurement error was calculated by using the interclass correlation coefficient on the 12 repeat measurements for CL, CW, and CH.

RESULTS

For 3D linear measurement groups, significant differences were found between the direct measurements and CBCT measurements for the CL group at W7 and W8, and for the CW group at W6, W7, and W8. No significant measurement differences were found for the CH group. The average linear measurements for CL, CW, and CH along with the direct measurement (DM) are shown in Table 6.

With respect to the CL0 and CL1 groups, a significant difference was found in percent volume at windows 9, 10, 17, 18, 19, 21, and 22 (Figure 5). For the

Table 3. Definitions of Anatomic Landmarks

Landmark	Definition
Anterior mandibular condyle (ACo)	Most anterior extent of the mandibular condyle viewed from the anterior, medial, lateral, and superior planes of view
Posterior mandibular condyle (PCo)	Most posterior extent of the mandibular condyle viewed from the posterior, medial, lateral, and superior planes of view
Lateral mandibular condyle (LCo)	Most lateral extent of the mandibular condyle viewed from the anterior, posterior, lateral, and superior planes of view
Medial mandibular condyle (MCo)	Most medial extent of the mandibular condyle viewed from the anterior, posterior, medial, and superior planes of view
Superior mandibular condyle (SCo)	Most superior aspect of the mandibular condyle viewed from the anterior, posterior, medial, lateral, and superior planes of view
Lingula (L)	Apex of the lingula

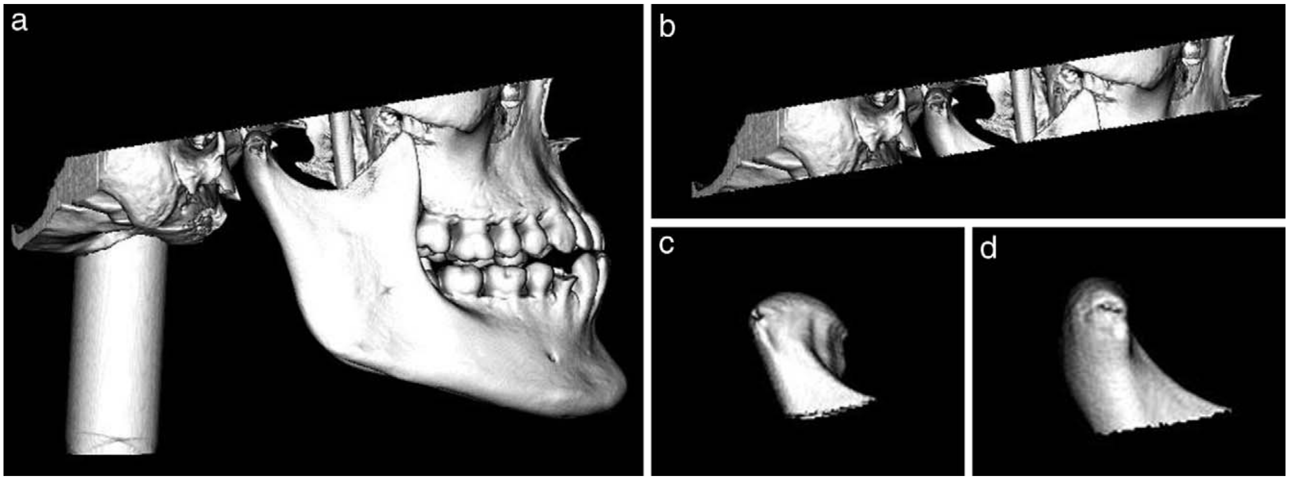

Figure 3. 3D reconstruction isolation for volumetric measurements of the mandibular condyle: (a) initial cut parallel to Frankfort horizontal, (b) second cut parallel to the first cut at the level of the most inferior point in the sigmoid notch, and (c,d) oblique and lateral views of the final isolated reconstruction.

CW0 and CW1 groups significant differences were found in WW 1–9 and 15–21 (Figure 6).

Table 7 lists independent *t*-test results and significance for CL0 compared with CL1, and CW0 compared with CW1. CL0 and CW0 groups demonstrated greater percent volumes in the higher density windows than the corresponding CL1 and CW1 groups.

The inverse relationship was evident in the lower density windows (Figures 5 and 6). So generally, the condyles that showed the greatest linear measurement change in W8 (176 to 2476 HU) were those with a higher percentage of low bone mineral density (BMD), while those with little change in measurement from the gold standard appear to have an increased BMD content.

Linear measurement reliability was tested using the intraclass correlation coefficient (ICC). Repeat measurements were accomplished on 12 condyles for all three linear measurements. A Cronbach alpha of 0.917 was found for the ICC test (ICC $>$ .80 is acceptable).

Table 4. Hounsfield Unit Window Widths (WW) Used to Create 3D Condyle Renderings for Volumetric Evaluation (Window 24 is Equal to the Sum of Window Widths 1–23)

Window Widths (WW) for Volumetric Evaluation	
WW 1	176 to 275 HU
WW 2	276 to 375 HU
WW 3	376 to 475 HU
WW 4	476 to 575 HU
WW 5	576 to 675 HU
WW 6	676 to 775 HU
WW 7	776 to 875 HU
WW 8	876 to 975 HU
WW 9	976 to 1075 HU
WW 10	1076 to 1175 HU
WW 11	1176 to 1275 HU
WW 12	1276 to 1375 HU
WW 13	1376 to 1475 HU
WW 14	1476 to 1575 HU
WW 15	1576 to 1675 HU
WW 16	1676 to 1775 HU
WW 17	1776 to 1875 HU
WW 18	1876 to 1975 HU
WW 19	1976 to 2075 HU
WW 20	2076 to 2175 HU
WW 21	2176 to 2275 HU
WW 22	2276 to 2375 HU
WW 23	2376 to 2475 HU
WW 24	176 to 2475 HU

DISCUSSION

Studies have shown that CT images can be remarkably accurate for linear,[3,16–18] geometric,[19] and volumetric[20] measurements within the maxillofacial complex.

The purpose of the present study was not to test the accuracy of linear measurements made on the 3D reconstruction, but instead, to utilize its proven accuracy for the purposes of measuring the changes that occur in the condyle because of variation in reconstruction HU window level and window width. Window level and width variation for the 3D linear measurements did have a significant effect on the condylar width and length; however, changes in height were statistically insignificant. For this reason, CH was excluded from the volumetric comparison groups. CW was most profoundly affected by window level and width. Medial and lateral poles of the 3D condylar reconstructions were often the first to exhibit areas of erosion, thereby producing reduced CW measurements.

Significance was found in the following ranges: W6, W7, and W8. W8 (176 to 2476 HU) is the recommended window width for viewing bone with V-works

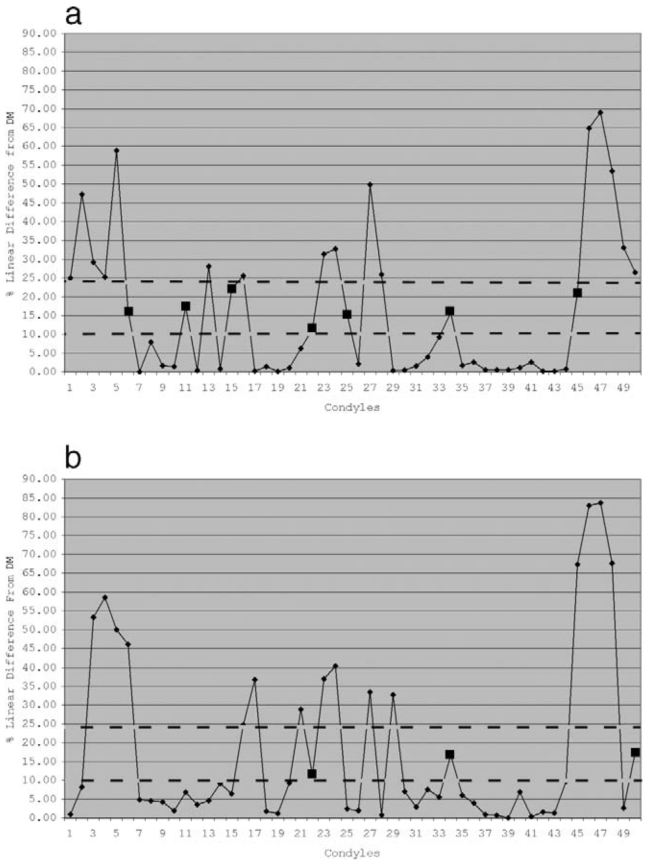

Figure 4. Distribution of percent differences between 3D linear measurements and direct measurement (DM); (a) condylar width (CW) measurement percent differences in W8 (176 to 2476 HU) with mean group (black square) between the dotted lines and (b) condylar length (CL) measurement differences in W8 with mean group (black square) between the dotted lines.

4.0. CL proved to be a challenging dimension to measure. ICC reliability testing showed measurement reproducibility to be acceptable; however, the extent of erosion was difficult to measure with point to point, and point to plane measurements. This likely resulted in fewer windows with significant measurement differences. Therefore, the CL was possibly more profoundly affected by changes in window level than the results indicate.

The Hounsfield unit has been used to describe physical density and achieve reasonable volume estimates of anatomic structures.[10–12,20,21] A number of studies have been performed in efforts to quantify bone density based on Hounsfield values.[10–12] Many of these studies were accomplished in order to help classify bone types best suitable to support dental implants.[10,11,14] For the present study, HU window widths and levels are manipulated in order to create 3D reconstructions most representative of the anatomic truth. For CW and CL the most accurate windows were below the recommended window for bone, and extended into the soft tissue range[22] as defined in Table 8. In a dry skull, extending into the soft tissue range will enhance visualization. However, in vivo the soft tissue will begin to appear and reduce one's capacity to view the bony topography. This would suggest that

Table 5. The Percent Volumes of the Condyles in the Outlying Groups

Window Width	CL1 (>25%)	CL0 (<10%)	CW1 (>25%)	CW0 (<10%)
WW 1	11.619	9.928	12.697	9.468
WW 2	9.606	8.678	10.288	8.414
WW 3	8.136	7.612	8.618	7.730
WW 4	7.064	6.726	7.298	6.872
WW 5	6.287	5.986	6.429	6.108
WW 6	5.662	5.323	5.728	5.428
WW 7	5.174	4.876	5.156	4.962
WW 8	4.921	4.522	4.837	4.626
WW 9	4.581	4.184	4.473	4.281
WW 10	4.348	4.009	4.191	4.143
WW 11	4.121	3.863	3.987	4.021
WW 12	3.869	3.750	3.723	3.909
WW 13	3.651	3.682	3.508	3.864
WW 14	3.453	3.541	3.249	3.757
WW 15	3.283	3.517	3.075	3.726
WW 16	3.071	3.535	2.849	3.759
WW 17	2.853	3.528	2.581	3.804
WW 18	2.540	3.322	2.211	3.655
WW 19	2.130	2.913	1.733	3.352
WW 20	1.686	2.450	1.264	2.921
WW 21	1.126	1.930	0.929	2.262
WW 22	0.566	1.339	0.706	1.423
WW 23	0.319	0.788	0.532	0.747

CL1: Greatest change in condylar length.
CL0: Least change in condylar length.
CW1: Greatest change in condylar width.
CW0: Least change in condylar width.

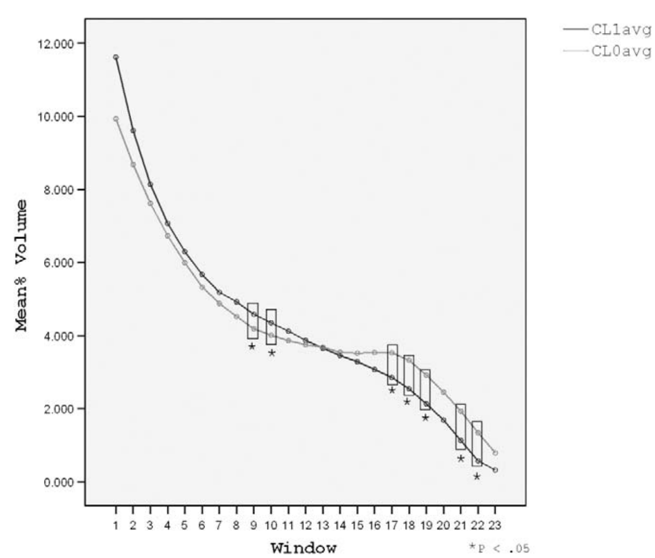

Figure 5. Distributions of condylar volume in 23 window widths for the condyles of groups CL1 and CL0; WW 1 represents the lowest density bone and WW 23 the highest density bone observed.

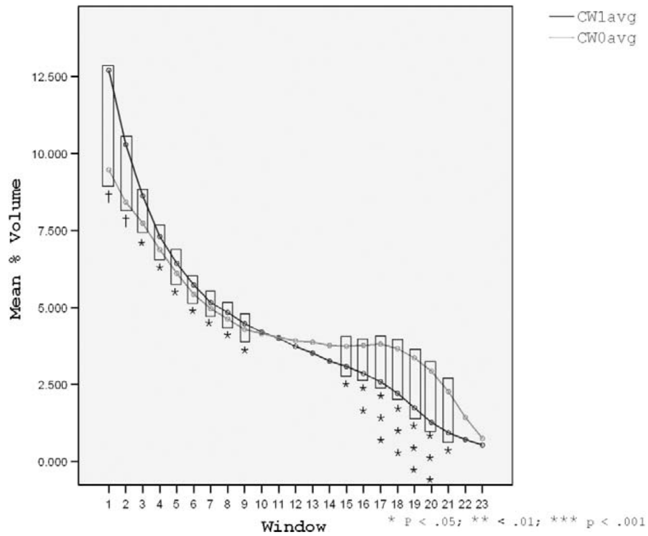

Figure 6. Distributions of condylar volume in 23 window widths for the condyles of groups CW1 and CW0; WW 1 represents the lowest density bone and WW 23 the highest density bone observed.

the CBCT 3D reconstructed image by itself may not be a reliable way to diagnose condylar pathology and changes in condylar morphology.

Though there was significant measurement change in W8 for CL and CW groups, there was a range of variation within each group for the 50 condyles. Some condyles exhibited large change while others showed little or no change at all. It is important to define why these condyles are different from each other. Is an increased difference in linear measurements from the anatomic truth directly related to the BMD composition of the condyle? The purpose of defining the volumetric distribution of BMD within the condyles was intended to answer this very question. The two groups compared graphically in Figures 5 and 6 show the volumetric distribution over 23 density ranges.

Significant differences in bone density distribution were found for both the CL and CW groups. Windows of significant difference were in the high- and low-density ranges. No significant differences were found in the midrange windows. The number of significant windows was greater for the CW0/CW1 group than the CL0/CL1 group. One would expect the CW and CL density distributions to be alike. They do follow the same pattern; however, the CL demonstrated fewer windows of significance between the CL0 and CL1 groups. This could relate to the difficulty presented in measuring morphologic defects in this dimension. In-

Table 7. Comparison (Independent *t*-Tests) of Volumetric Measurements: CL0 vs CL1, and CW0 vs CW1 at 23 Window Levels[a]

Volumetric Window	CL0 vs CL1		CW0 vs CW1	
	t	Sig	*t*	Sig
WW 1	−1.682	.100	3.417	.001**
WW 2	−1.386	.173	2.925	.006**
WW 3	−1.152	.255	2.637	.012*
WW 4	−1.072	.289	2.165	.036*
WW 5	−1.309	.197	2.489	.017*
WW 6	−1.707	.095	2.697	.010*
WW 7	−1.626	.111	2.265	.029*
WW 8	−2.247	.030*	2.296	.027*
WW 9	−2.358	.023*	2.211	.033*
WW 10	−1.972	.055	1.197	.238
WW 11	−1.597	.117	.690	.494
WW 12	−.742	.462	−.246	.807
WW 13	.174	.863	−1.154	.255
WW 14	.435	.665	−1.819	.076
WW 15	1.044	.302	−2.350	.024*
WW 16	1.812	.077	−3.287	.002**
WW 17	2.323	.025*	−4.210	.000***
WW 18	2.323	.025*	−4.333	.000***
WW 19	2.091	.042*	−4.403	.000***
WW 20	1.861	.069	−4.133	.000***
WW 21	2.038	.047*	−3.292	.002**
WW 22	2.288	.027*	−1.909	.063
WW 23	1.543	.130	−.586	.561

[a] Sig indicates significance.
* $P < .05$; ** $P < .01$; $P < .001$.

Table 6. Hounsfield Unit Window Widths (W) Used to Create 3D Condyle Renderings for Linear Measurements (Table 2 for W ranges). Average Condylar Length (CL), Condylar Width (CW), and Condylar Height (CH) Are Compared With the Direct Measurement (DM)

Comparison of CBCT Mean Linear Measurements to Gold Standard[a]									
Linear Measurement Windows	DM-CL, mm	CL, mm	Sig	DM-CW, mm	CW, mm	Sig	DM-CH, mm	CH, mm	Sig
W1	8.90	9.43	.058	18.50	19.10	.169	37.94	38.66	.590
W2	8.90	9.36	.098	18.50	18.90	.359	37.94	38.39	.736
W3	8.90	9.30	.149	18.50	18.65	.726	37.94	38.28	.800
W4	8.90	9.16	.342	18.50	18.24	.587	37.94	38.22	.832
W5	8.90	8.90	.988	18.50	17.67	.104	37.94	38.20	.849
W6	8.90	8.62	.442	18.50	16.78**	.004	37.94	38.15	.877
W7	8.90	8.08*	.040	18.50	15.66***	.000	37.94	38.06	.927
W8	8.90	7.72**	.006	18.50	15.66***	.000	37.94	37.62	.825

[a] Sig indicates significance.
* $P < .05$; ** $P < .01$; $P < .001$.

Table 8. Window Widths for Density Values and Hounsfield Numbers in the Body[22]

Part	Low Density Value[a]	High Density Value[a]
Air	0 (−1024)	500 (−524)
Skin	700 (−324)	1100 (−76)
Bone	1200 (176)	3500 (2476)
Tooth	2500 (1476)	4095 (3071)
Metal	3000 (1976)	4095 (3071)

[a] Parenthetic value is Hounsfield number.

capacity to record accurately the anatomic changes occurring across the range of HU windows could produce error in condyle selection for the CL0 and CL1 groups, thereby producing a volumetric comparison between two groups of condyles with very little variation between them.

The goal of this study was not to define the range of bone mineral densities that constitute the condyle. A study of this nature would require a sample of untreated cadaver condyles. Even then, research has shown that, HU are only reliable as BMD predictors in full trabecular bone, or in the presence of minimal cortical bone. HU readings from CT scans with thicker cortical bone become less reliable.[12,13] Also, CT numbers cannot be accepted as an absolute for characterization of a tissue type or lesion.[23] CT numbers may vary significantly from one scanner to another, or even between two scanners of the same make and model.[23,24]

However, with some degree of success, standardized calibration methods have been employed in efforts to minimize interscan discrepancies.[25] With attention to detail, strict standardization in all parameters, continual manufacturer support, and application of proper calibration methods, reproducibility can be optimized.[26] Studies focused on CT numbers as an accurate representation of tissue density have, for the most part, been confined to conventional CT scanners. Recently, Aranyarachkul et al[10] examined variations in bone density in designated implant recipient sites using both CBCT and conventional CT. They found both modalities to be consistent in their measurements of bone density value, but the values were generally higher for CBCT. Whether CBCT or conventional CT values are closer to corresponding histologic bone densities has yet to be investigated.

CONCLUSIONS

- Assessment of the mandibular condyle, using the 3D reconstruction, is most accurate when accomplished at density levels below that recommended for osseous examination.

REFERENCES

1. Brooks SL, et al. Imaging of the temporomandibular joint: a position paper of the American Academy of Oral and Maxillofacial Radiology. *Oral Surg Oral Med Oral Pathol Oral Radiol Endod.* 1997;83:609–618.
2. Sukovic P. Cone beam computed tomography in craniofacial imaging. *Orthod Craniofac Res.* 2003;6(suppl 1):31–36; discussion 179–182.
3. Hilgers ML, Scarfe WC, Scheetz JP, Farman AG. Accuracy of linear temporomandibular joint measurements with cone beam computed tomography and digital cephalometric radiography. *Am J Orthod Dentofacial Orthop.* 2005;128:803–811.
4. Mah JK, Danforth RA, Bumann A, Hatcher D. Radiation absorbed in maxillofacial imaging with a new dental computed tomography device. *Oral Surg Oral Med Oral Pathol Oral Radiol Endod.* 2003;96:508–513.
5. Honda K, Larheim TA, Maruhashi K, Matsumoto K, Iwai K. Osseous abnormalities of the mandibular condyle: diagnostic reliability of cone beam computed tomography compared with helical computed tomography based on an autopsy material. *Dentomaxillofac Radiol.* 2006;35:152–157.
6. Kau CH, Richmond S, Palomo JM, Hans MG. Three-dimensional cone beam computerized tomography in orthodontics. *J Orthod.* 2005;32:282–293.
7. Hatcher DC, Aboudara CL. Diagnosis goes digital. *Am J Orthod Dentofacial Orthop.* 2004;125:512–515.
8. Ludlow JB, Davies-Ludlow LE, Brooks SL, Howerton WB. Dosimetry of 3 CBCT devices for oral and maxillofacial radiology: CB Mercuray, NewTom 3G and i-CAT. *Dentomaxillofac Radiol.* 2006;35:219–226.
9. Walker L, Enciso R, Mah J. Three-dimensional localization of maxillary canines with cone-beam computed tomography. *Am J Orthod Dentofacial Orthop.* 2005;128:418–423.
10. Aranyarachkul P, et al. Bone density assessments of dental implant sites: 2. Quantitative cone-beam computerized tomography. *Int J Oral Maxillofac Implants.* 2005;20:416–424.
11. Shapurian T, Damoulis PD, Reiser GM, Griffin TJ, Rand WM. Quantitative evaluation of bone density using the Hounsfield index. *Int J Oral Maxillofac Implants.* 2006;21:290–297.
12. Stoppie N, Pattijn V, Van Cleynenbreugel T, Wevers M, Vander Sloten J, Ignace N. Structural and radiological parameters for the characterization of jawbone. *Clin Oral Implants Res.* 2006;17:124–133.
13. Rho JY, Hobatho MC, Ashman RB. Relations of mechanical properties to density and CT numbers in human bone. *Med Eng Phys.* 1995;17:347–355.
14. Hatcher DC, Dial C, Mayorga C. Cone beam CT for presurgical assessment of implant sites. *J Calif Dent Assoc.* 2003;31:825–833.
15. Hounsfield GN. Nobel Award address. Computed medical imaging. *Med Phys.* 1980;7:283–290.
16. Lascala CA, Panella J, Marques MM. Analysis of the accuracy of linear measurements obtained by cone beam computed tomography (CBCT-NewTom). *Dentomaxillofac Radiol.* 2004;33:291–294.
17. Kobayashi K, Shimoda S, Nakagawa Y, Yamamoto A. Accuracy in measurement of distance using limited cone-beam computerized tomography. *Int J Oral Maxillofac Implants.* 2004;19:228–231.
18. Misch KA, Yi ES, Sarment DP. Accuracy of cone beam computed tomography for periodontal defect measurements. *J Periodontol.* 2006;77:1261–1266.
19. Marmulla R, Wortche R, Muhling J, Hassfeld S. Geometric

accuracy of the NewTom 9000 Cone Beam CT. *Dentomaxillofac Radiol.* 2005;34:28–31.
20. Breiman RS, et al. Volume determinations using computed tomography. *AJR Am J Roentgenol.* 1982;138:329–333.
21. Kobayashi F, Ito J, Hayashi T, Maeda T. A study of volumetric visualization and quantitative evaluation of bone trabeculae in helical CT. *Dentomaxillofac Radiol.* 2003;32:181–185.
22. Cybermed. Imaging software for real time 3D visualization. In: *V-Works_4.0 Manual*. Chapter 6. Common Tools, 36. Seoul, Korea: Cybermed Co, Ltd: 2006.
23. Levi C, Gray JE, McCullough EC, Hattery RR. The unreliability of CT numbers as absolute values. *AJR Am J Roentgenol.* 1982;139:443–447.
24. Stadler A, et al. CT density measurements for characterization of adrenal tumors ex vivo: variability among three CT scanners. *AJR Am J Roentgenol.* 2004;182:671–675.
25. Cann CE. Quantitative CT for determination of bone mineral density: a review. *Radiology.* 1988;166:509–522.
26. Cann CE. Quantitative CT applications: comparison of current scanners. *Radiology.* 1987;162:257–261.